A Simple Model for Simulation of Particle Deaggregation of Few-Particle Aggregates

Erik Kaunisto and Anders Rasmuson
Dept. of Chemical Engineering, Chalmers University of Technology, Gothenburg SE-412 96, Sweden

Johan Bergenholtz
Dept. of Chemistry and Molecular Biology, University of Gothenburg, Gothenburg SE-412 96, Sweden

Johan Remmelgas, Lennart Lindfors, and Staffan Folestad
AstraZeneca R&D, Mölndal SE-431 83, Sweden

DOI 10.1002/aic.14363
Published online January 27, 2014 in Wiley Online Library (wileyonlinelibrary.com)

A proper mechanistic understanding of the deaggregation process of small colloidal particle aggregates is of generic importance within many fields of science and engineering. The methodology for modeling colloidal deaggregation is currently limited to analytical solutions in the two-particle case and time consuming numerical algorithms, such as Brownian Dynamics (BD) simulations, for many-particle aggregates. To address this issue, a simplified alternative model that describes deaggregation of few-particle aggregates is presented. The model includes end-particle deaggregation and a particle reconfiguration mechanism, which are the two most important mechanisms for deaggregation. Comparison of the calculated first passage time distribution for various two-, three-, four-, and five-particle aggregates with the corresponding result using BD simulations confirms the validity of the model. It is concluded that the dominating mechanism behind deaggregation can be quantified using a deaggregation number, which reflects the time scale for reconfiguration relative to the time scale for end-particle deaggregation. © 2014 American Institute of Chemical Engineers *AIChE J*, 60: 1863–1869, 2014

Keywords: colloids (ionic systems in water), diffusion, mathematical modeling, particle technology

Introduction

Deaggregation of colloidal species plays an important role in many engineering fields, for example, drug release from tablet formulations,[1] subsurface transport of contaminants,[2] filtration, bioremediation, and water treatment.[3] In contrast to aggregation, the fundamental mechanisms behind deaggregation are currently not well understood. However, earlier work on agglomeration in milling processes has shown that the stability factor, which accounts for electrostatic and van der Waals interactions between particles, seems to play an important role.[4] Similarly, a recent pharmaceutical study has shown that the addition of ionic surfactant at subcritical micelle concentrations enhances drug dissolution from drug particle aggregates, making the dissolution process approach that of a nonaggregated system.[5] These findings both suggest that colloidal interactions and DLVO theory,[6,7] may provide at least a partial qualitative explanation of the deaggregation process.

Colloidal interactions and stability are mainstay topics of research within colloid science and they have been extensively studied in the literature. Based on the theory of hydrodynamically interacting Brownian particles[8] and the Smoluchowski equation, that are relevant for describing the dynamics of colloidal-size particles, Chan and Halle[9] derived an analytical expression for the so-called mean first passage time (MFPT), that is, the mean time it takes for two particles to deaggregate, for a pair of weakly flocculated particles subject to, for example, a DLVO interaction-potential. A similar mathematical treatment related to diffusion-controlled reactions has also been presented by Szabo et al.,[10] from which also the full first passage time distribution (FPTD) can be obtained. Unfortunately, these methods are in practice limited to two-particle aggregates and cannot be directly applied to study more general many-particle aggregates. An alternative methodology that can be used in these cases is Brownian dynamics (BD) simulations.[11] In a recent study by Kaunisto et al.,[1] it was found that BD simulations can be used to calculate and analyze FPTD:s and MFPT:s of three- and four-particle aggregates. Kaunisto et al.[1] also found that BD simulations are very time consuming and quickly become infeasible as the number of particles increases. The general applicability of BD simulations is thus limited and computationally less expensive models are required.

The objective of this work is to develop a simplified model for deaggregation of small particle aggregates that can replace otherwise time and resource consuming BD simulations. For this purpose, this work is based upon a previous result due to Kaunisto et al.,[1] who found that deaggregation of at least small aggregates seems to be governed mainly by

Correspondence concerning this article should be addressed to A. Rasmuson at rasmuson@chalmers.se.

relatively loosely bound initial end-particles as well as a particle reconfiguration mechanism. The new model combines these two mechanistic assumptions, where end-particle deaggregation is based on an extension of the two-particle "on-off" dissociation dynamics approach by Bergenholtz et al.[12] and reconfiguration is regarded as a simple diffusion process. The model is used to calculate FPTD:s of polystyrene particles in water, which are compared with those obtained from BD simulations for compact two-, three-, four-, and five-particle aggregates (densely packed particles) and non-compact three-, four-, and five-particle aggregates (non-densely packed particles). Further, the impact of the particle interaction-potential on the FPTD:s is studied and the relative importance of initial end-particle deaggregation and reconfiguration is discussed.

Theory

Model for deaggregation of two particles

This work is based on first passage time theory approach for colloidal two-particle aggregates.[9,10] Neglecting hydrodynamic interactions, this framework allows for the diffusing and interacting identical particles to be described by the two-particle adjoint Smoluchowski equation for the survival probability, $\Sigma(\tau|x)$, Eq. 1, subject to a no-flux boundary condition at a short separation x_a and an absorbing boundary condition at the separation distance x_b

$$\frac{\partial\Sigma(\tau|x)}{\partial\tau}=\frac{1}{x^2}e^{\beta u(x)}\frac{\partial}{\partial x}\left(x^2e^{-\beta u(x)}\frac{\partial\Sigma(\tau|x)}{\partial x}\right)$$
$$\tau=\frac{2D_0t}{\sigma^2},\ x=\frac{r}{\sigma},\ \beta=\frac{1}{k_bT},\ D_0=\frac{k_bT}{3\pi\eta\sigma} \tag{1}$$

where $u(x)$ (J) is the pair-interaction potential, D_0 $(\mathrm{m^2/s})$ is the single-particle diffusion coefficient (Stokes–Einstein), t (s) is the time, σ (m) is the particle diameter, r (m) is the center-to-center distance between the particles, k_b (J/K) is the Boltzmann constant, T (K) is the temperature, and η (kg/m/s) is the shear viscosity of the suspending fluid. The survival probability describes the likelihood that a pair of particles, initially separated by x, have not deaggregated by time τ and can be used to obtain the FPTD, $\varrho(\tau|x)=-\frac{\partial\Sigma(\tau|x)}{\partial\tau}$ and MFPT, $\bar{\tau}=\int_0^\infty\tau\varrho(\tau|x)d\tau$. Equation 1 can generally only be solved numerically, but in the case of the MFPT, the closed-form expression by Chan and Halle,[9] Eq. 2, can also be used

$$\bar{\tau}=\int_x^{x_b}dyy^{-2}e^{\beta u(y)}\int_{x_a}^{y}dss^2e^{-\beta u(s)} \tag{2}$$

Even though the FPTD cannot be obtained analytically in the general case, there has been significant progress. For example, in a recent article by Bergenholtz et al.,[12] the solution to Eq. 1 using a square-well pair-interaction potential in the Baxter limit[13] is discussed. It turns out that for strongly adhesive particles the long-time dynamics of the solution completely dominates, leading to a survival probability and a FPTD given by Eqs. 3 and 4, respectively

$$\Sigma(\tau|1)\approx e^{-a_1^2\tau} \tag{3}$$

$$\varrho(\tau|1)\approx a_1^2e^{-a_1^2\tau} \tag{4}$$

$$\tan\left[\alpha_m(x_b-1)\right]=\frac{12\tau_s\alpha_m}{12\tau_s-\alpha_m^2} \tag{5}$$

where α_1 is the eigenvalue governing the long-time dynamics, defined as the smallest of the eigenvalues, α_m, satisfying Eq. 5, where τ_s is the Baxter stickiness parameter. Small values of τ_s correspond to strong adhesive interactions between the particles and in these cases the FPTD:s obtained from solving Eq. 1 with a DLVO potential and Eq. 4, respectively, show the same qualitative features.[12] It is, therefore, argued that the physics of the DLVO potential can be mapped onto the Baxter parameter by matching the MFPT from Eq. 2 with the corresponding expression in the Baxter limit, Eq. 6[12]

$$\bar{\tau}=\frac{1}{6}\left(x_b^2-1\right)+\frac{1-x_b}{3x_b}\left(1-\frac{1}{4\tau_s}\right) \tag{6}$$

Further, as the FPTD according to Eq. 4 is an exponential distribution, it can be interpreted as a Poisson process where the dynamics is governed by a constant probability. In the limit of small time steps, the distribution can thus be reconstructed from a simple coin-flip process, where the probability $p\ll1$ to deaggregate during an arbitrary but sufficiently small time step $\Delta\tau$ is given by Eq. 7[12]

$$p=a_1^2\Delta\tau$$
$$\Delta\tau=\frac{2D_0\Delta t}{\sigma^2} \tag{7}$$

As shown above, the coin-flip model offers a tractable way of simplifying the two-particle deaggregation process without a significant loss of physical understanding or accuracy. In this work, the possibility to expand upon this approach to describe deaggregation of two-, three-, four-, and five-particle aggregates is examined.

The particle interaction potential

The particle interactions are taken to be described by a fluid-averaged isotropic DLVO pair-interaction-potential of mean force. The interactions consist of both attractive van der Waals forces and repulsive electrostatic forces and can be modeled using the linear superposition approximation.[1,14] In this work, the DLVO parameters correspond to spherical polystyrene particles with a radius of 3 μm in water, using $\psi_0=50$ mV for the surface potential, $c_n=1.3,\ 2.0,\ 2.8$ mM, for the 1:1 electrolyte concentrations, $A=1.3\times10^{-20}$ J for the Hamaker constant,[15] $\varepsilon_r=80$ for the dielectric constant of water and $T=298.15$ K. The different potentials are shown in Figure 1.

Based on previous work,[1,9,16] the FPTD in the case of reversible aggregation can be based on the time it takes for a particle to escape the secondary minimum, as shown in Figure 1. Using the definition by Kaunisto et al.,[1] the particles are considered deaggregated when they have reached $x_b>x$ with an interaction energy equal to 1 k_bT, which represents the typical energy of thermal fluctuations. The resulting calculated eigenvalues were $\alpha_1=3.8006,\ 1.3898,\ 0.4920$ for $c_n=1.3,\ 2.0,\ 2.8$ mM, respectively.

Model for deaggregation of small aggregates

A common approach to describe colloidal particle displacements on the Smoluchowski time scale is to use BD simulations.[11] As previously mentioned, the study by Kaunisto et al.[1]

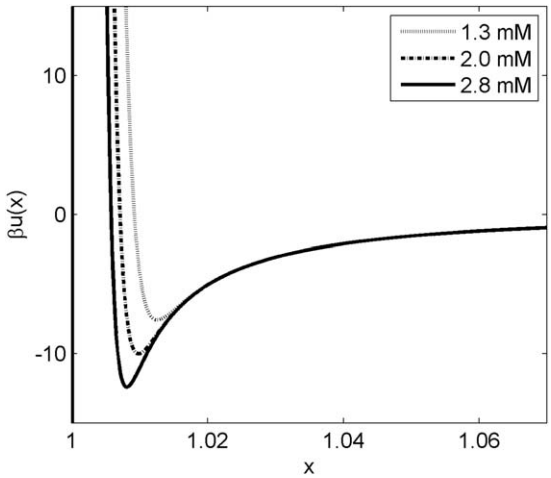

Figure 1. The DLVO pair-interaction potentials for the different 1:1 electrolyte concentrations studied.

The corresponding primary energy barriers at small center-to-center separation distances are visible. The secondary minima are located at approximately $x=$ 1.0126, 1.0098, 1.0081 with corresponding well depths of $u_{min}=7.6$, 10, $12.4k_bT$ for $c_n=1.3$, 2.0, 2.8 mM, respectively.

demonstrated that the BD algorithm can be used to calculate both FPTD:s and MFPT:s and thus provide an understanding of the deaggregation process of three- and four-particle aggregates. Conversely, a BD algorithm quickly becomes infeasible as the number of particles increases due to the computational effort required. One way to address this issue is to develop an alternative and computationally efficient model that can replace a BD model by only taking the most important mechanisms of deaggregation into account. As concluded by Kaunisto et al.,[1] the two most important mechanisms appears to be deaggregation of loosely bound initial end-particles and reconfiguration, where the former can be approximately described as a two-particle deaggregation process. If end-particle deaggregation is relatively slow, reconfiguration may transform an initially noncompact aggregate (nondensely packed particles) into a compact aggregate (densely packed particles) with an increased amount of particle interactions which delays deaggregation.

It is reasonable to assume that the total probability p_1 to deaggregate an end-particle from a noncompact aggregate during a time step $\Delta\tau$ is proportional to the number of initial end-particles n_e. As each end-particle in turn can be approximated by the two-particle case, Eq. 8 is a logical extension of Eq. 7 that accounts for the fact that an n-particle aggregate can have more than one end-particle. Analogously, if the aggregate is compact the deaggregation process is governed by the number of most weakly bound particles n_e^* and the number of particle neighbors, according to Eq. 9, where $\Delta\tilde{\tau}$ is a modified time step and k is the neighbor coefficient. The neighbor coefficient is to be interpreted as the effective number of particle interactions for the most weakly bound particles in a compact aggregate. Further, in order to account for the reconfiguration mechanism for noncompact aggregates, a simple diffusion process is used, Eq. 10, where d_{old} and d are the equipotential distances traveled before and after the latest time step, respectively, and $\boldsymbol{n}$ is a Gaussian random number from the unit normal distribution. The aggregate is assumed to be compact when the absolute traversed diffusion distance $|d|$ reaches the critical value d_c

$$p_1 = n_e p = n_e \alpha_1^2 \Delta\tau \tag{8}$$

$$p_2 = n_e^* p^k = n_e^* \alpha_1^{2k} \Delta\tilde{\tau} \tag{9}$$

$$d = d_{old} + \sqrt{\sigma^2 \Delta\tau} * \boldsymbol{n} \tag{10}$$

Using a convenient acronym, the combined algorithm based on Eqs. 8–10 will in this work be referred to as A Simple Algorithm for Peptization (ASAP) model and can be schematically summarized as follows:

1. **for** number of trajectories
2. Update τ
3. **if** aggregate status = noncompact $\rightarrow X=p_1$
4. Update d
   if $|d| \geq d_c \rightarrow$ aggregate status = compact
5. **if** aggregate status = compact $\rightarrow X=p_2$
6. **if** random number $[0,1] < X \rightarrow$ save τ
   else goto 2
7. reset aggregate status
   goto 1

The ASAP algorithm was implemented in Fortran 77 and run on an Intel Xeon W3530 2.80 GHz processor in a system with 12 GB RAM memory to generate independent trajectories for the FPTD:s of the aggregates studied. The corresponding BD simulations were also performed on a computer cluster, as previously described by Kaunisto et al.[1] The CPU time for the ASAP model was typically on the order of seconds to hours, depending on desired accuracy. For the BD simulations, the corresponding times were on the order of minutes to days, using 1000 CPU cores.

Results and Discussion

Two-particle model validation

To check the validity of the coin-flip assumption, the results for the two-particle model by Bergenholtz et al.[12] were compared with the results from the corresponding BD simulation, by setting $p_1=p$ in the ASAP model. The scenario corresponds to a specific situation with one end-particle, that is, $n_e=1$, which is due to the fact that both particles deaggregate simultaneously and thus cannot be distinguished between. The simulations were carried out with parameters corresponding to a 1:1 electrolyte concentration of 2 mM, using a time step $\Delta\tau=0.001$ and a time step tolerance (i.e., the time step governing parameter of the BD simulation)[1] of $\delta=0.001$ for the ASAP model and the BD simulation, respectively. The number of trajectories was 5000 for the BD simulation and 20,000 for the ASAP model. The time step and time step tolerance were chosen to be sufficiently small not to have any significant effect on the results.

In the BD simulations,[1] the time step was sufficiently small to resolve particle diffusion and interaction on the high primary energy barrier (see Figure 1), and it was, therefore, not necessary to include a bounce-back criterion explicitly. That is, in the BD simulations, the time step was sufficiently small for the barrier itself to act as a natural bounce-back criterion. A bounce-back criterion is included in the ASAP model using a no-flux boundary condition at a short separation distance and an absorbing boundary condition at a larger separation, as explained by Bergenholtz et al.[12] This latter

separation distance was chosen so that the total particle interaction energy at the separation distance was the same in the BD simulation as in the ASAP model.

The FPTD:s are shown in Figure 2, where probability distribution function is plotted vs. the first passage time. As can be seen in Figure 2, the FPTD:s from the ASAP model and BD simulation are in good agreement. The time step and time step tolerance correspond to real time steps of approximately 0.2 s and 40 μs for the ASAP model and the BD simulation, respectively. The ASAP model thus gives results with the same accuracy as the BD simulation model but using a time step that is larger than the BD time step by a factor of almost 10^4, which clearly demonstrates the efficiency of the ASAP model.

Model comparison for three-, four-, and five-particle aggregates

Using the same time step, tolerance, and number of trajectories as in the two-particle case, the ASAP and BD models were also applied to study different three-, four-, and five-particle aggregates. Figure 3 shows the FPTD:s from the three-particle aggregates. For the compact triangular aggregate shown in Figure 3A, the ASAP model shows the same unimodal distribution characteristics as the BD simulation. However, tuning the ASAP model to give agreement with the BD simulation model requires a neighbor coefficient of $k \approx 1.88$, which is slightly less than the value that can be anticipated based upon the number of neighbors of the most weakly bound particles, that is, $k=2$. The effective number of particle neighbors is thus less than expected, most likely due to the simultaneous movement of all particles. This latter effect, which is a many-body effect, is not taken into account in the ASAP model. Conversely, as can be seen in Figures 3B, C the same value of $k=1.88$ was used to predict the position of the late-stage peaks of the bimodal distributions for linear and L-shaped aggregates, thus further validating the ASAP model. Further, in Figure 3B, the early stage peaks are in good agreement and are slightly shifted toward early times, as compared to Figure 2. This can be explained by the multiplicity of the end-particles, that is, $n_e=2$, in the three-particle case, resulting in a higher probability for deaggregation than in the two-particle case. The relative intensities of the early stage and late-stage peaks are captured, at least qualitatively, by assuming a representative critical

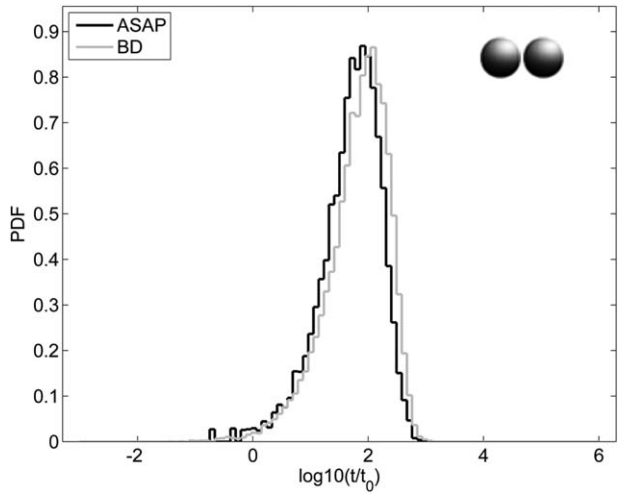

Figure 2. FPTD:s obtained from using a time step $\Delta\tau=0.001$ and a time step tolerance of $\delta=0.001$ for the ASAP model and the BD simulation, respectively, for a two-particle aggregate with $c_n=2.0$ mM and $t_0=1$ s.

The number of trajectories was 5000 for the BD simulation and 20,000 for the ASAP model.

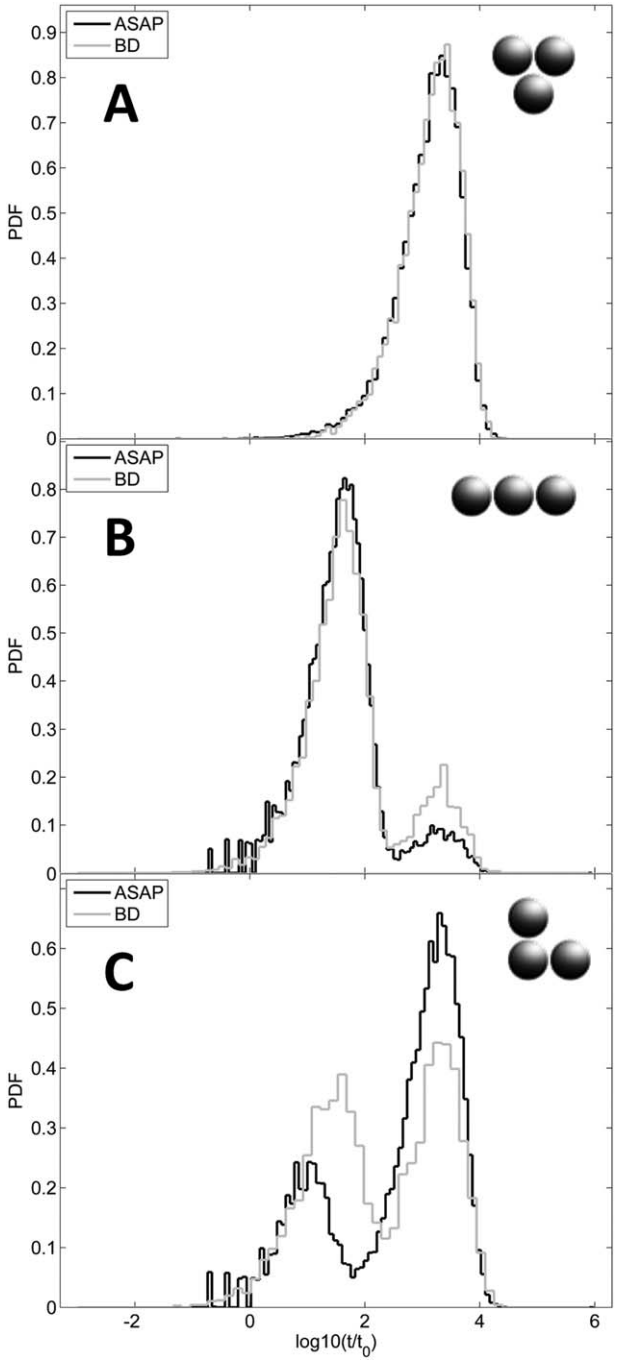

Figure 3. FPTD:s obtained from using a time step $\Delta\tau=0.001$ and a time step tolerance of $\delta=0.001$ for the ASAP model and the BD simulation, respectively, for different three-particle aggregates with $c_n=2.0$ mM and $t_0=1$ s.

(A) Compact triangular aggregate with $n_e^*=3$ and $k=1.88$ (unimodal distribution). (B) Noncompact linear aggregate with $n_e=2$, $k=1.88$, and $d_c=\frac{\pi\sigma}{3}$ (bimodal distribution). (C) Noncompact L-shaped aggregate with $n_e=2$, $k=1.88$, and $d_c=\frac{\pi\sigma}{12}$ (bimodal distribution).

diffusion distance corresponding to the least amount of total equipotential movement required for the two initial end-particles to come in contact and form a compact aggregate. The shorter the diffusion distance the larger the intensity of the late-stage peak and vice versa.

For the aggregates depicted in Figures 3B, C, the diffusion distance d_c can be roughly estimated by considering diffusion of the end particles around the middle particle. Thus, for the aggregates in Figures 3B, C, the diffusion distance can be roughly estimated as $d_c = \frac{\pi\sigma}{3}$ and $d_c = \frac{\pi\sigma}{12}$, respectively, which is simply the product of half the minimal total tangential movement required for particle contact and the particle diameter. We emphasize that this merely is a rough estimate and that a better estimate in this particular case may be obtained by considering diffusion of a particle on a spherical surface with an absorbing boundary at some azimuthal coordinate, $\phi = \phi_c$, where the absorbing boundary represents the other end particle. In such a representation, the diffusing end particle starts at zero, and the configurations in Figures 3B, C then correspond to $\phi_c = \frac{2\pi}{3}$ and $\phi_c = \frac{2\pi}{6}$, respectively. Although such a consideration is expected to have no effect on the results for the configuration in Figure 3B, it is clear that it will result in a larger value of d_c and possibly better agreement with the results from the BD simulations for the configuration in Figure 3C. This issue is interesting in itself, but we emphasize that it is an issue that is limited to the particular case in Figure 3C and that the rough estimate of d_c works surprisingly well in all other cases considered, including the four- and five-particle aggregates considered below.

In addition, unlike the BD model, the ASAP model assumes that the middle particle is static. A possible explanation for the differences between the two models in Figures 3B, C is, therefore, that movement of the middle-particle has an effect on the end particles in the BD model, whereas it does not in the ASAP model. For example, initial movement of the middle-particle for the aggregate in Figure 3B perpendicular to the axis of the aggregate maintains the same center-to-center distance with both end-particles. However, diffusion of the end particles is promoted in the direction of the secondary minimum, that is, toward the center of the middle particle, which implies that the motion of the end particles in this new configuration has a component which causes the end particles to move toward each other, thus promoting reconfiguration to a compact cluster. Using this simple example, it is thus easy to understand that the middle particle has an effect that will tend to delay deaggregation in the BD model relative to the ASAP model, which is in agreement with the results in Figure 3B. It is not in agreement with the result in Figure 3C, though we have already noted that this discrepancy most likely is due to a less than optimal choice of the diffusion distance in Figure 3C.

The FPTD:s obtained from the four-particle aggregates are shown in Figure 4. The deaggregation process of the tetrahedral aggregate in Figure 4A yields the same type of unimodal distribution as for the triangular aggregate in Figure 3A. The value of the neighbor coefficient that is required to obtain agreement between the ASAP and BD models is $k \approx 2.53$, which is less than the expected value of $k=3$. Similar to the three-particle case, this value of k was also used to predict the bimodal FPTD:s of the linear and propeller-shaped aggregates in Figures 4B, C, respectively. Compared to the three-particle case, the critical diffusion distance for the linear four-particle aggregate is more difficult to estimate as it is not obvious how this aggregate reconfigures into a more compact form. However, as can be seen in Figure 4B, assuming similar diffusion distances turns out to be a good approximation. For the propeller-shaped aggregate in Figure 4C, the shortest required diffusion distance required for two end-particles to meet, that is, $d_c = \frac{\pi\sigma}{6}$, seems to be a good approximation.

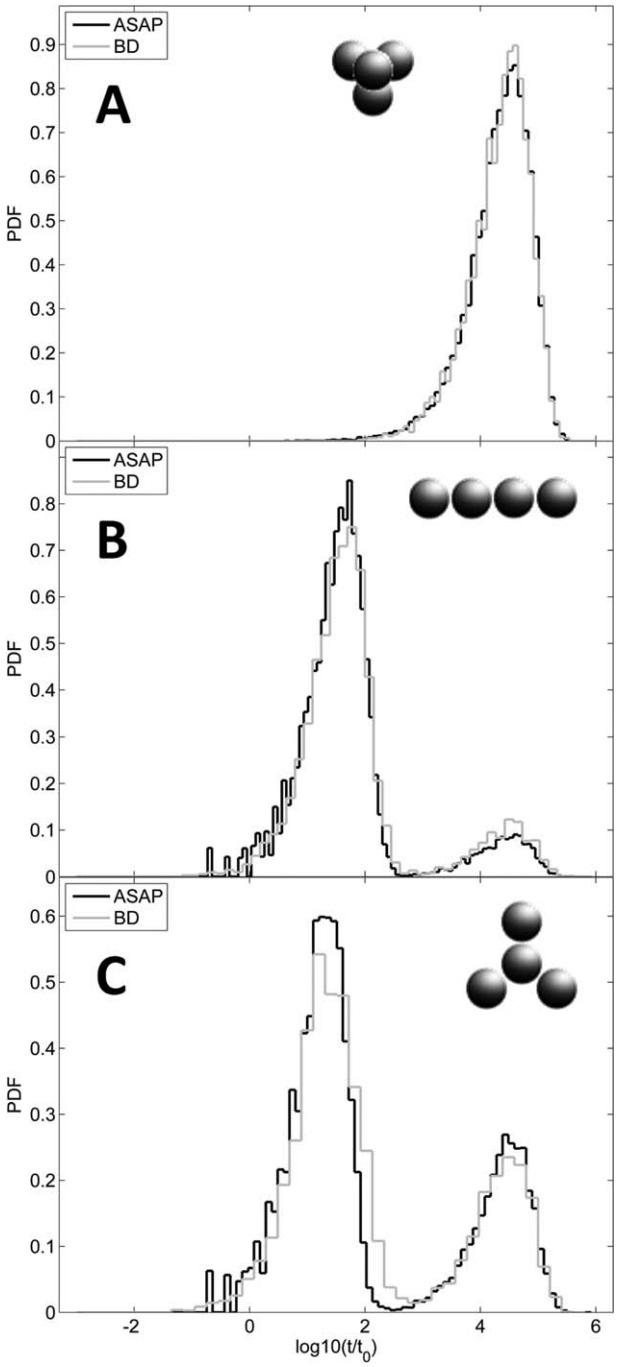

Figure 4. FPTD:s obtained from using a time step $\Delta\tau = 0.001$ and a time step tolerance of $\delta = 0.001$ for the ASAP model and the BD simulation, respectively, for different four-particle aggregates with $c_n = 2.0$ mM and $t_0 = 1$ s.

(A) Compact tetrahedral aggregate with $n_e^* = 4$ and $k = 2.53$ (unimodal distribution). (B) Noncompact linear aggregate with $n_e = 2$, $k = 2.53$, and $d_c = \frac{\pi\sigma}{3}$ (bimodal distribution). (C) Noncompact propeller-shaped aggregate with $n_e = 3$, $k = 2.53$, and $d_c = \frac{\pi\sigma}{6}$ (bimodal distribution).

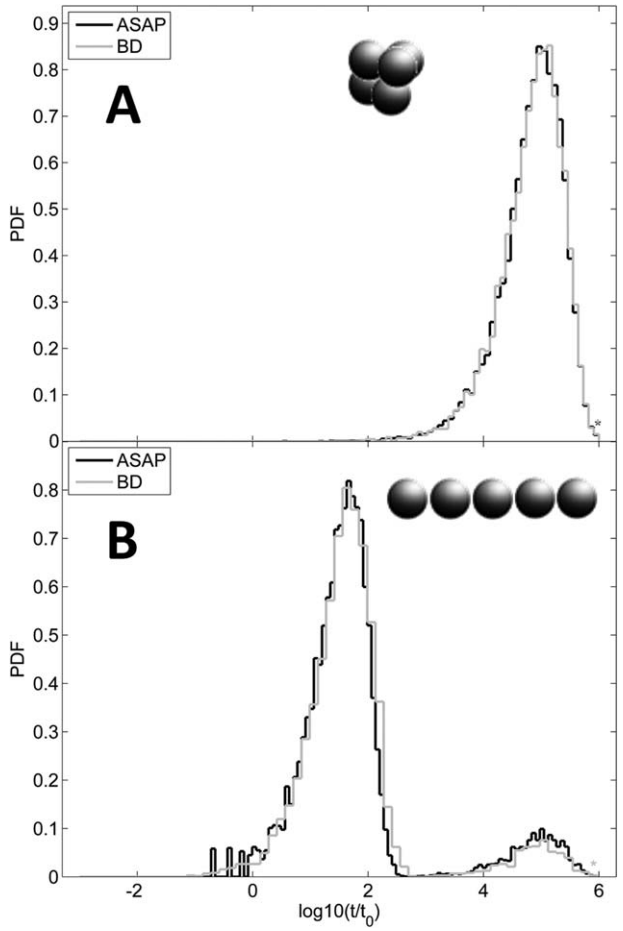

Figure 5. FPTD:s obtained from using a time step $\Delta\tau = 0.001$ and a time step tolerance of $\delta = 0.001$ for the ASAP model and the BD simulation, respectively, for two five-particle aggregates with $c_n = 2.0$ mM and $t_0 = 1$ s.

(A) Compact triangular dipyramid-shaped aggregate with $n_e^* = 2$ and $k = 2.63$ (unimodal distribution). (B) Noncompact linear aggregate with $n_e = 2$, $k = 2.63$, and $d_c = \frac{\pi\sigma}{3}$ (bimodal distribution).

As can be seen in Figure 5, the ASAP model was also compared with BD simulations in the five-particle case. Figure 5A shows the FPTD:s obtained from a triangular dipyramid-shaped aggregate. In this aggregate, the two most weakly bound particles have three neighbors, whereas the remaining three particles have four neighbors. For $n_e^* = 2$, the required value of the neighbor coefficient for agreement between the two models is $k \approx 2.63$. This value of the neighbor coefficient is similar to that of the tetrahedral aggregate in Figure 4A, suggesting that the two most weakly bound particles in the triangular dipyramid-shaped aggregate play the most important role in governing the deaggregation process. As in the previous cases, the FPTD of the linear five-particle aggregate shown in Figure 5B was calculated using the same diffusion distance as in the three- and four-particle cases.

When comparing the compact three-, four-, and five-particle aggregates, it is worth noting that the value of the neighbor coefficient is smaller than the expected value for all aggregates. In addition, it differs less from the expected value for the five-particle aggregate than for the four-particle aggregate. As the number of neighbors and the number of particles with which a particle can interact is limited even for many-particle aggregates, the trend observed in the value of the neighbor coefficient as more particles are added suggests that an asymptotic value of the neighbor coefficient may exist for compact many-particle aggregates. Although this asymptotic value obviously cannot be determined from the limited simulation data in this work, the small difference in the value of the neighbor coefficient between the four- and five-particle aggregates may indicate rapid convergence to the asymptotic value as more particles are added. Further research is, however, needed to establish whether such an asymptotic value exists, which requires simulations of particle aggregates that contain far more than four or five particles.

Effect of the pair-interaction potential on deaggregation

In the previous section, it was shown that the intensities of the early stage and late-stage peaks in the bimodal distribution of a noncompact aggregate can be related to the diffusion distance. However, the relative intensity of these peaks also depends on the pair-interaction potential. To explore the effect of the interaction potential on the deaggregation process, simulations are also carried out for parameters that correspond to a 1:1 electrolyte concentration of $c_n = 1.3$ mM and $c_n = 2.8$ mM.

Figures 6A, B show the FPTDs for the linear three-particle aggregate for 1:1 electrolyte concentrations of $c_n = 1.3$ mM and $c_n = 2.8$ mM, respectively. As can be seen in Figure 6, there is a significant mechanistic shift in the deaggregation process of the linear three-particle aggregate for the electrolyte concentrations considered. From Figure 1, it can be seen that a lower electrolyte concentration implies a shallower energy minimum, in which case end-particle deaggregation will govern the deaggregation process and the reconfiguration mechanism will be insignificant. This explains the unimodal distribution in Figure 6A. Conversely, if the electrolyte concentration is higher, the energy minimum will be deeper and the end-particles will be more strongly bound. In this case, the aggregate will have time to reconfigure to a more compact form, which explains the bimodal distribution in Figure 6B. Thus, the importance of end-particle deaggregation relative to reconfiguration depends on the time scale for deaggregation compared to the time scale for reconfiguration. Assuming that the MFPT in the two-particle case, that is, Eq. 2, can represent the time scale for end-particle deaggregation and that the time scale for diffusion can be estimated based on the concept of diffusion length,[17] implying $d_c = \sqrt{4D_0 t_c}$, where t_c is the time required to reach d_c, a dimensionless deaggregation number, N, can be defined according to Eq. 11. With this definition

$$N = \frac{\bar{\tau}}{\tau_c} = \frac{2\sigma^2 \int_x^{x_b} dy y^{-2} e^{\beta u(y)} \int_{x_a}^{y} ds s^2 e^{-\beta u(s)}}{d_c^2} \qquad (11)$$

$$\tau_c = \frac{2D_0 t_c}{\sigma^2} = \frac{d_c^2}{2\sigma^2}$$

$N \ll 1$ means that the end-particle deaggregation process dominates, whereas for $N \gg 1$ reconfiguration is more important. For the linear three-particle aggregate, the deaggregation numbers for $c_n = 1.3,\ 2.0,\ 2.8$ mM are $N = 0.13,\ 0.94,\ 7.53$, respectively. The FPTD:s in Figures 3B and 6A, B are thus straightforward to understand.

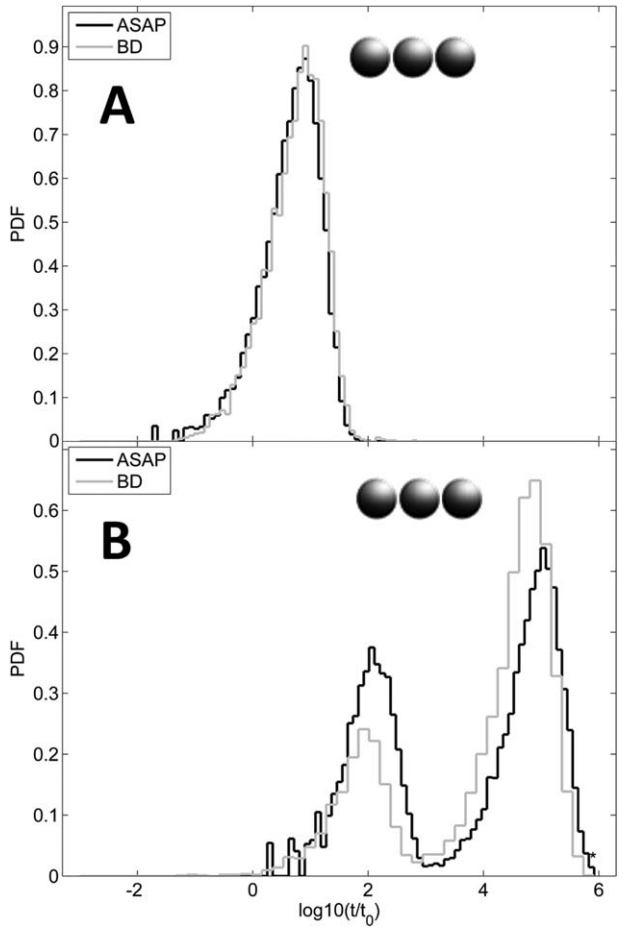

Figure 6. FPTD:s obtained from using a time step $\Delta\tau = 0.001$ and a time step tolerance of $\delta = 0.001$ for the ASAP model and the BD simulation, respectively, for a linear three-particle aggregate with $n_e = 2$, $k = 1.88$, $d_c = \frac{\pi\sigma}{3}$, and $t_0 = 1$ s.

(A) $c_n = 1.3$ mM (unimodal distribution). (B) $c_n = 2.8$ mM (bimodal distribution).

Conclusions

In this study, a computationally efficient model that describes deaggregation of small compact and noncompact colloidal aggregates has been developed. This model, which is referred to as the ASAP model, was used to calculate and analyze FPTD:s from different two-, three-, four-, and five-particle aggregates. The results were found to be in qualitative agreement with results from corresponding BD simulations. From the results, it was concluded that the two most important features governing the deaggreation process can be attributed to an end-particle detachment process on the one hand and a particle reconfiguration mechanism on the other. The relative importance of these two mechanisms can be estimated from their relative time scales. It was shown that the time scale for reconfiguration is related to a critical equipotential diffusion distance, whereas the time scale for end-particle deaggregation depends on the pair-interaction potential.

As the number of particle neighbors is limited even in many-particle aggregates, deaggregation from large aggregates may be expected not to depend critically on the number of particles in the aggregate. Although this work is limited only to two-, three-, four-, and five-particle aggregates, the results obtained indicate that an asymptotic behavior is obtained as more particles are added to the aggregates; further work is needed to establish whether this indeed is the case.

Acknowledgment

AstraZeneca is gratefully acknowledged for funding this project.

Literature Cited

1. Kaunisto E, Rasmuson A, Bergenholtz J, Remmelgas J, Lindfors L, Folestad S. Fundamental mechanisms for tablet dissolution: simulation of particle deaggregation via brownian dynamics. *J Pharm Sci*. 2013;102(5):1569–1577.
2. McCarthy JF, Zachara JM. Subsurface transport of contaminants. *Environ Sci Technol*. 1989;23(5):496–502.
3. Loveland JP, Ryan JN, Amy GL, Harvey RW. The reversibility of virus attachment to mineral surfaces. *Colloids Surf A*. 1996;107:205–221.
4. Sommer M, Stenger F, Peukert W, Wagner NJ. Agglomeration and breakage of nanoparticles in stirred media mills—a comparison of different methods and models. *Chem Eng Sci*. 2006;61(1):135–148.
5. Jonsson M. *Modeling Hydrodynamic Effects of Drug Dissolution and Deaggregation of Low Soluble Compounds in the Small Intestine* [M. Sc.]. Linköping University, Linköping, 2010.
6. Verwey EJW, Overbeek JTG. *Theory of the Stability of Lyophobic Colloids*. New York: Elsevier Publishing Company, Inc., 1948.
7. Derjaguin BV, Landau L. Theory of the Stability of Strongly Charged Lyophobic Sols and of the Adhesion of Strongly Charged Particles in Solutions of Electrolytes. *Acta Phys Chim URSS*. 1941; 14:633–662.
8. Batchelor GK. Brownian diffusion of particles with hydrodynamic interaction. *J Fluid Mech*. 1976;74(1):1–29.
9. Chan DYC, Halle B. Dissociation kinetics of secondary-minimum flocculated colloidal particles. *J Colloid Interface Sci*. 1984;102(2): 400–409.
10. Szabo A, Schulten K, Schulten Z. First passage time approach to diffusion controlled reactions. *J Chem Phys*. 1980;72(8):4350–4357.
11. Ermak DL, McCammon JA. Brownian dynamics with hydrodynamic interactions. *J Chem Phys*. 1978;69(4):1352–1360.
12. Bergenholtz J, Kaunisto E, Rasmuson A, Remmelgas J, Folestad S, Lindfors L. On-off dissociation dynamics of colloidal doublets. *Europhys Lett*. 2013;104(1):18005.
13. Baxter RJ. Percus–Yevick equation for hard spheres with surface adhesion. *J Chem Phys*. 1968;49(6):2770–2774.
14. Russel WB, Saville DA, Schowalter DR. *Colloidal Dispersions*. Cambridge: Cambridge University Press, 1989.
15. Parsegian VA, Weiss GH. Spectroscopic parameters for computation of van der waals forces. *J Colloid Interface Sci*. 1981;81(1):285–289.
16. Bacon J, Dickinson E, Parker R, Anastasiou N, Lal M. Motion of flocs of two or three interacting colloidal particles in a hydrodynamic medium. *J Chem Soc Faraday Trans 2*. 1983;79(1):91–109.
17. Bird RB, Stewart WE, Lightfoot EN. *Transport Phenomena*, *2nd ed.* New York: Wiley, 2007.

Manuscript received Sept. 2, 2013, and revision received Dec. 6, 2013.